Silicon (2022) 14:6457–6465
https://doi.org/10.1007/s12633-021-01441-5

ORIGINAL PAPER

Mechanical and Thermodynamic Characteristics of $22SiO_2$-$23Bi_2O_3$-$37B_2O3$-$13TiO_2$-(5-x) LiF- x BaO Glasses

Kh. S. Shaaban[1] · Z. A. Alrowaili[2] · Ateyyah M. Al-Baradi[3] · Atif Mossad Ali[4,5] · E. A. Abdel Wahab[6] · M. S. Al-Buriahi[7]

Received: 26 August 2021 / Accepted: 18 September 2021 / Published online: 7 October 2021

Abstract
The glass system $22SiO_2$- $23Bi_2O_3$-$37B_2O_3$-$13TiO_2 - (5 - x)$ LiF- x BaO, $(0 \leq x \leq 5)$mol.%. was fabricated using melt-quenching techniques. X-ray diffraction and ultrasonic techniques were used to characterize the glasses. X-ray diffraction patterns were used to prove that fabricated glasses are amorphous. The impacts of incorporating BaO on the composition dependence of the elastic characteristics of fabricated samples were explained. Density of the manufacture glasses increment, and molar volume reduced. The elastic moduli were investigated experimentally then compared using theoretical arguments. Makishima – Mazinize model were used to determine the elastic moduli theoretically for fabricated samples. Elastic moduli increase with BaO, and experimental and theoretical elastic moduli are in good agreement. Deviation values between elastic moduli (both experimentally and theoretically) were estimated. All the experimental variations values of elastic moduli of fabricated glasses were increment as BaO increased. Latent heat of melting, diffusion constant, and Grüneisen factor have been used to link the mechanical and thermodynamic characteristics of manufactured glass.

Keywords Mechanical · Elastic modulus · Hardness · Diffusion constant · Grüneisen factor

1 Introduction

Excellent mechanical, thermal, optics, and radiation characteristics attract researchers to titanate borosilicate glasses. As a result, titanate borosilicate glasses are among the most thoroughly investigated. These glasses are doped with different transition metal oxides (TMO) and form dense glass networks. Theoretical and experimental methods were used by many physicists and chemists to investigate these glasses [1–12]. Because of its exceptional mechanical characteristics, glass with (TMO) has been used in a variety of applications in recent decades [13–16].

TiO_2 is a common glass preservative that is used to enhance the glass' mechanical and radiation characteristics. Glass scientists are interested in TiO_2 because small amounts of it can have a big impact on mechanical and shielding characteristics [17–22]. TiO_2 is important in glass systems because of its various coordination states Ti^{+4}, Ti^{+5}, and Ti^{+6}. Because of the change in coordination, TiO_2 can have a completely different effect on the characteristics [17–22].

Glasses manufactured of BaO-TiO_2-SiO_2-B_2O_3 have an appealing structure for observing changes in glass behavior, as well as LiF-TiO_2-SiO_2-B_2O_3 glasses, represent the same behavior [23–25]. As a result of its high dielectric constant and chemical stability, another glass system, titanium barium borosilicate glass, is being investigated. Mechanical and radiation properties of titanium barium borosilicate glass have been discovered to be useful. Shen et al. [26] investigated the structural characteristics of titanium barium silicate glass after doping it with La_2O_3. In the titanium barium silicate

✉ Kh. S. Shaaban
khamies1078@yahoo.com

1 Chemistry Department, Faculty of Science, Al-Azhar University, P.O. Box 71524, Assiut, Egypt

2 Physics Department, College of Science, Jouf University, P.O. Box: 2014, Sakaka, Saudi Arabia

3 Department of Physics, College of Science, Taif University, P.O. Box 11099, Taif 21944, Saudi Arabia

4 Physics Department, Faculty of Science, King Khalid University, 61413 Abha, Saudi Arabia

5 Department of Physics, Faculty of Science, Assiut University, 71516 Assiut, Egypt

6 Physics Department, Faculty of Science, Al Azhar University, P.O. Box 71524, Assiut, Egypt

7 Department of Physics, Sakarya University, Sakarya, Turkey

glass, Komori et al. [27] added a provides an appropriate of Nb_2O_5. Rammah et al. [28] investigate the structural and shielding characteristics of the TeO_2-$LiNbO_3$-BaO-BaF_2-La_2O_3 glass system. El Batal et al. [29] investigate the NaF-CaF_2-B_2O_3 glass system's structural and gamma irradiation influence. The effects of La_2O_3 on the mechanical, and radiation characteristics of NaF - BaO - PbO - B_2O3 glasses were studied by Abd El-Rehim [30] and Shaaban et al. [31].

The fabricated glasses were examination using mechanical techniques. The impact of increasing BaO content on mechanical features has been investigated.

2 Materials and Methods

The glass system $22SiO_2$- $23Bi_2O_3$-$37B_2O_3$-$13TiO_2$ $-(5-x)$ LiF- x BaO, $(0 \le x \le 5)$mol.%. in Table 1 was fabricated using melt-quenching techniques. H_3BO_3 is transformed into B_2O_3 and H_2O evaporation. The reactants were blended and melted in ceramic crucibles for 2 h at 1200 °C in an electric furnace. At 450 °C, the manufactured samples were annealed.

A Philips X-ray diffractometer (model PW/1710) that used to examine the samples' condition. The glass density was calculated using the Archimedes principle and CCl_4 as the buoyant medium.

Ni content calculated $N_i = \left(\frac{6.023\times10^{23}x\ mol\ fraction\ of\ cation\times\ valency\ of\ cation}{Vm}\right)$,inter-ionic distance, $R_i = \left(\frac{1}{\text{Concentrationof Ni}}\right)^{\frac{1}{3}}$, polaron radius r_p and internuclear distance r_i, determined as, $rp = \frac{1}{2}\left(\frac{\pi}{6N}\right)^{\frac{1}{3}}$, $ri = \left(\frac{1}{N}\right)^{\frac{1}{3}}$. Ba – Ba separation computed as $(\text{dBa}-\text{Ba}) = \left(\frac{V_m^B}{N}\right)^{\frac{1}{3}}$ and $V_m^B = \frac{Vm}{2(1-2Xn)}$, average number coordinated $m = \sum n_{ci}X_i$. The number of bonds as $n_b = \frac{N_A}{V_m}\sum n_{ci}X_i$. Mechanical constraints in total $N_{con} = N_{bs} + N_{bb}$ where N_{bb} is bond bending constraints and N_{bs} is bond stretching, $N_{bb} = \frac{\sum xim}{2}, N_{bs} = \sum xi(2m-3)$. Considering floppy modes $M_f = 2 - \frac{5m}{6}$, density of cross-linking D_{CL} as $D_{cl} = N_{con} - 2$,

Table 1 The glass constitution of the investigated samples

Sample code	SiO_2	Bi_2O_3	B_2O_3	TiO_2	LiF	BaO
	mol.%.					
G 1	22	23	37	13	5	0
G 2	22	23	37	13	4	1
G 3	22	23	37	13	3	2
G 4	22	23	37	13	2	3
G 5	22	23	37	13	0	5

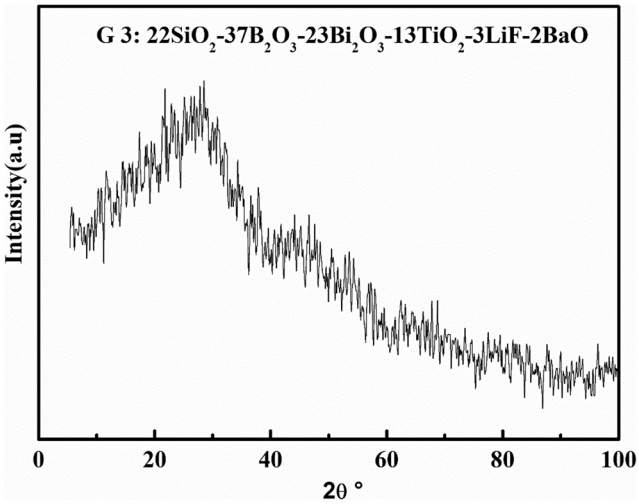

Fig. 1 XRD of manufactured samples

$CN_{eff} = \frac{2}{5}N_{con} + 3$. Cohesive energy (CE) is calculated using a formula CE (*Kcal /mol*) = 18.17+.

$4.53E_{opt}$, or (*e.V /atom*) = 0.792 + $0.198E_{opt}$ (eV). The predictable network volume (N_v) and network connectivity (N_c) are as [32].

Ultrasonic velocities were determined using a pulse-echo procedure (Echograph model 1085), repeated the experiments three-time. Elastic moduli (longitudinal waves L, transverse waves G, young's modulus Y, and bulk modulus K) are calculated using velocities in addition to density as $L = \rho v_l^2$, $G = \rho v_t^2$, $Y = (1+\sigma)2G$, and $K = L - \left(\frac{4}{3}\right)G$. Using the concept of packing density V_i and dissociation energy G_i, the elastic moduli of the samples can be evaluated [33, 34]. Fractal bond conductivity $d = \left(G/K\right) * 4$.

$Vi = \left(\frac{3\pi}{4}\right)N_A(m\text{R}_\text{A}{}^3 + \text{nR}_\text{O}{}^3)\text{m}^3.\text{mol}^{-1}$, and $Gi = \left(\frac{1}{V_m}\right)\sum_i GiXi$, metallic elements and oxygen R_m and R_O are the Pauling ionic radii. According to this concept $L = K + \left(\frac{4}{3}\right)G$,

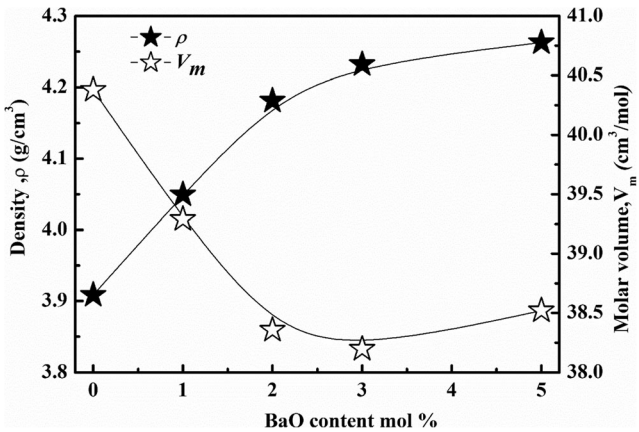

Fig. 2 ρ & *Vm* of manufactured samples

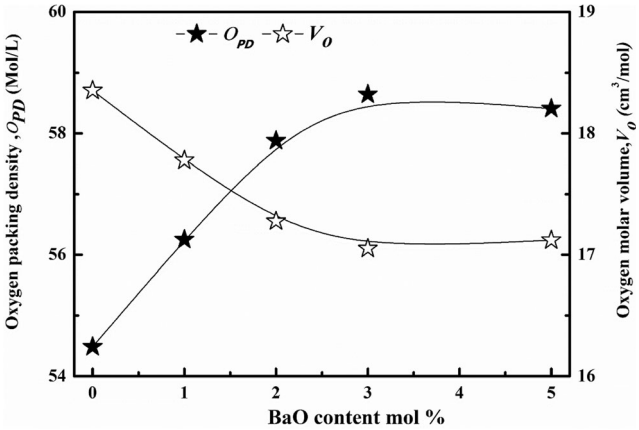

Fig. 3 *OPD* & *Vo* of fabricated glasses

$G = 30 * \left(\frac{V_i^2 G_i}{V_i}\right)$, $Y = 8.36 V_i G_i$, and $K = 10 V_i^2 G_i$. The ratio of Poisson's $\sigma = \frac{1}{2} - \left(\frac{1}{7.2 * Vi}\right)$. Impedance of the acoustic system; $Z = v_L \rho$. Hardness in microns; $H = \frac{(1-2\sigma)Y}{6(1+\sigma)}$. Temperature of Debye: $\theta_D = \frac{h}{k}\left(\frac{9N_A}{4\pi V_m}\right)^{\frac{1}{3}} M_s$, Where h, k and N_A are Planck's, Boltzmann's, and Avogadro's constants, respectively. Velocity averages $M_s = \frac{1}{3}\left(\frac{2}{v_T^3} + \frac{1}{v_l^3}\right)^{\frac{1}{3}}$. Coefficient of thermal $\alpha_{P=23.2(v_L - 0.57457)}$. Oxygen Molar Volume and Oxygen Packing Density $V_o = \left(\frac{M}{\rho}\right)\left(\frac{1}{\sum xini}\right)$, and $OPD = \left(\frac{1000C}{Vm}\right)\left(\frac{Mol}{L}\right)$. Diffusion constant D_i and the latent heat ΔH_m estimated as: $D_i = \frac{r_i^2 K\theta_D}{96h}$ and $\Delta H_m = \frac{9M}{128}\left(\frac{r_i K\theta_D}{h}\right)2$. The bond length is denoted by r_i and molar mass of the samples is M. Grüneisen parameter (ϒ) determined as $\Upsilon = \frac{9(V_L^2 - \frac{4V_L^2}{3})}{2(V_L^2 - 2V_T^2)}$.

Table 2 Physical characteristics of $22SiO_2$- $23Bi_2O_3$-$37B_2O_3$-$13TiO_2$-$(5-x)$ LiF- x BaO glasses

Samples	G 1		G 2	G 3	G 4	G 5
(Ni) (10^{21} ions/cm^3)	-		0.312	0.629	0.948	1.57
R_i (Å)	-		15.06	11.86	10.35	8.753
ri (Å)	-		17.347	13.7	11.96	10.13
r_p (Å)	-		4.98	3.93	3.43	2.91
(d_{Ba-Ba}), nm	0.58		0.573	0.566	0.564	0.561
(m)	4.82		4.84	4.86	4.88	4.92
n_b (10^{28} m^{-3})	7.19		7.42	7.63	7.69	7.69
N_{bs}	2.41		2.42	2.43	2.44	2.46
N_{bb}	3.32		3.34	3.36	3.38	3.42
$N_{con.}$	5.73		5.76	5.79	5.82	5.88
M_f		2.017	2.03	2.05	2.07	2.1
D_{CL}		3.73	3.76	3.79	3.82	3.88
CN_{eff}		5.292	5.304	5.316	5.328	5.352
cohesive energy, CE(Kcal/mol)		32.48	32.17	31.69	31.37	30.03
cohesive energy, CE (atom /e.V)		1.42	1.4	1.38	1.37	1.31

3 Results and Discussions

3.1 Physical Investigation

Figure 1 shows the XRD of manufactured glasses in the 2θ between (10–100). Only the XRD for $22SiO_2$- $23Bi_2O_3$-$37B_2O_3$-$13TiO_2$-3LiF-2BaO is shown here because the XRD of all manufactured glasses was similar. The hump in the synthesized glass in Fig. 1 indicates that it is non-crystalline because of the presence of short-range effects. Therefore, make sure the fabricated samples are amorphous [35–38].

Figure 2 depicted the measured density, ρ and molar volume, V_m. With an increase in BaO content, the density of glasses increased. Because of the higher molecular weights

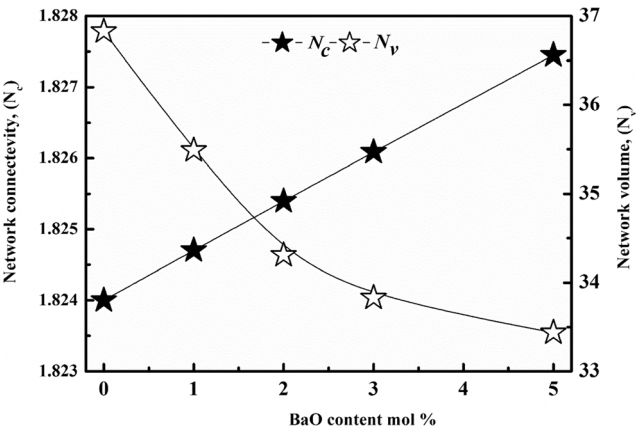

Fig. 4 N_c & N_v of fabricated glasses

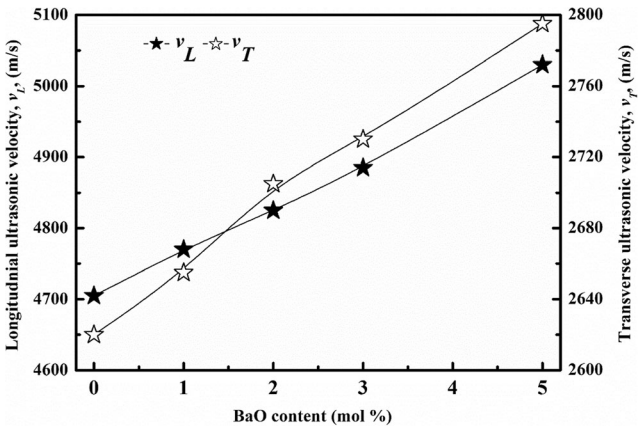

Fig. 5 V_L & V_T of fabricated glasses

Table 3 The values of (V_L), (V_T), and elastic moduli of $22SiO_2$-$23Bi_2O_3$-$37B_2O_3$-$13TiO_2$-$(5-x)$ LiF- x BaO glasses

Samples name	V_L (m. s^{-1})	V_T	L (GPa)	G	K	Y	L_{th}	G_{th}	K_{th}	Y_{th}
G 1	4705	2620	86.53	26.83	50.75	68.43	51.04	21.7	22.12	46.47
G 2	4770	2655	92.14	28.54	54.08	72.82	53.75	22.4	23.91	48.48
G 3	4825	2705	97.34	30.59	56.55	77.76	56.4	23.04	25.67	50.41
G 4	4885	2730	101	31.54	58.94	80.3	58.67	23.7	27.09	52.14
G 5	5030	2795	107.85	33.3	63.45	85.03	59.03	23.8	27.24	52.46

and density of BaO, (153.326 & 5.72), than LiF (25.939&2.64 g/cm^3), the result is easily explained.

With the addition of BaO, the Vm values were found to decrease. It was ascribed to the formation of a glass network because of an increase in the number of bridging oxygens (BO) in glass [39–43].

Similarly, as BaO increased, *OPD* values increased and *Vo* decreased. In fabricated glasses, Ba^{+2} has a lower field strength than LiF, which can result in an increase in (BO). Moreover, as the number of (BO) atoms risen, voluminous units incorporating end oxygen atoms reduced, resulting in an increment in OPD values and a decline in Vo. Figure 3 depicted OPD& Vo [44–48].

Figure 4 shows variation in N_c & N_v with BaO content, indicates that adding BaO has similar ρ & N_m effects. When compared to the parent composition, the structure contracted, and when BaO was added, the contraction effect was even stronger. The improvements in the glass connection can be seen in Figs. 2, 3 and 4. This result agrees with the others [47–51].

Because of the decrease in molar volume, the ion concentration (N_i) of Ba^{+2} rises. In this study, (R_i), (r_i), and (r_p) were calculated, and it was discovered that decreased as Ba^{+2} concentrations increased. This decrease was accompanied by a reduction in V_m. Due to the decline in V_m, the values of (dB a − Ba) increased with the concentration of Ba^{+2}.

(m) is a crucial parameter for determining whether the oxygen bond is bridging or not. It is discovered that Ba^{+2} increases the value of m increased, indicates that adding BaO has created (BO). These findings revealed that as the content of BaO increased, n_b increased as well. In the glass system, the role of a BaO modifier is illustrated. Table 2 summarizes the calculated values for these parameters [45–51].

$E_{opt.}$ values and *CE* have a direct proportional relationship. As a result, as BaO concentration rises, the cohesive energy values decrease. The values of $N_{con.}$, N_{bs}, and N_{bb} are approximated. With the increase in BaO, these parameters are reported to increase. With increment BaO, CN_{eff}, D_{CL}, and M_f values increase. Table 2 summarizes the calculated factors [48- 51].

3.2 Mechanical Characteristics

Figure 5 exemplifies the ultrasonic (longitudinal (V_L) and shear (V_T)) velocities for fabricated glasses at various BaO mole %. The propagation of both (V_L) and (V_T) velocities in bulk samples was responsible for changes in glass structure. The (V_L) and (V_T) were both increased as a result. This behaviour, indicating that BaO plays a dominant role in velocities in these glasses. The fact that the addition of BaO caused a rapid movement of the (V_L) and (V_T) inside the

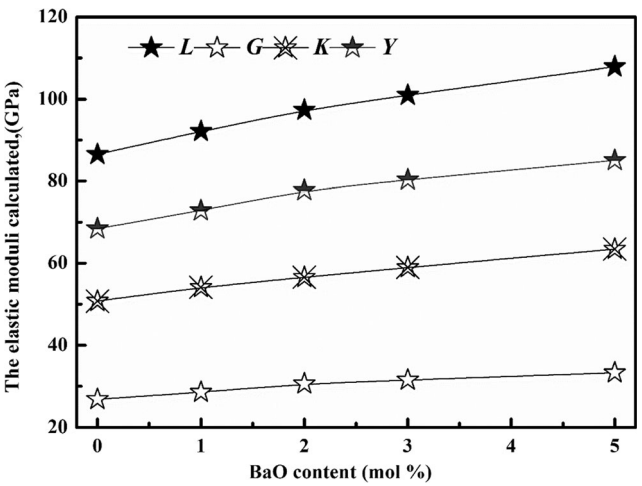

Fig. 6 L, G, K & Y elastic moduli experimentally of fabricated glasses

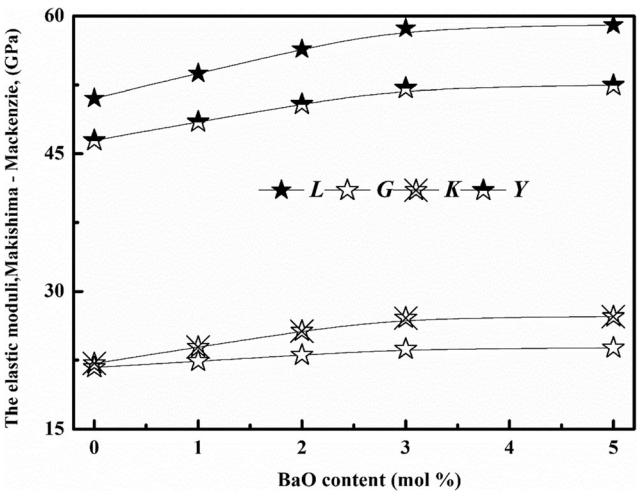

Fig. 7 L, G, K & Y elastic moduli theoretically of fabricated glasses

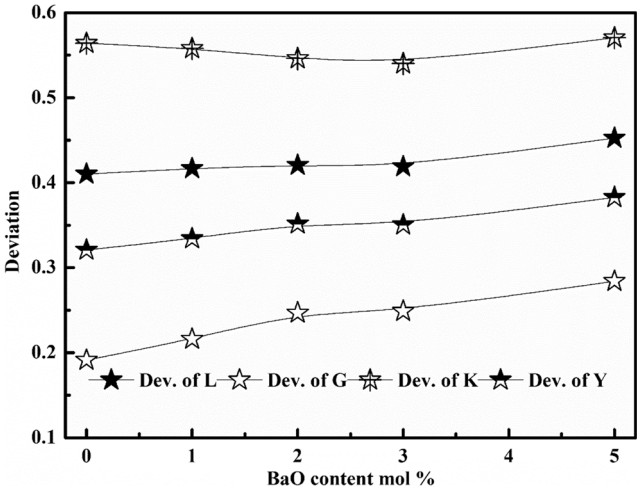

Fig. 8 *Diviation* of elastic moduli (experimentally & theoretically) of fabricated glasses

network of the glass structure was revealed by the increase in (V_L) and (V_T) of the considered glass. As BaO increased, (V_L) and (V_T) of these samples increased as well. Table 3 shows the values of (V_L), (V_T).

The elastic moduli (experimentally and theoretically) in this study behave in a similar way to (V_L) and (V_T), as shown in Figs. 6 and 7. The higher bond strength and the change in the coordination number of Ba-O than Li-F structural units caused an increase in elastic moduli as the BaO expanded. Addition BaO creates the glass structure more rigid, increasing the velocity and elastic moduli. Table 3 shows elastic moduli data.

The following are the estimated deviation values between elastic moduli (both experimentally and theoretically): Dev. $= \frac{(\text{elasticmoduli})_{ex} - \text{elasticmoduli})_{th}}{(\text{elasticmoduli})_{ex}}$. The deviation values of elastic moduli were demonstrated in Fig. 8. Elastic moduli increase with BaO, and experimental and theoretical elastic moduli are in good agreement.

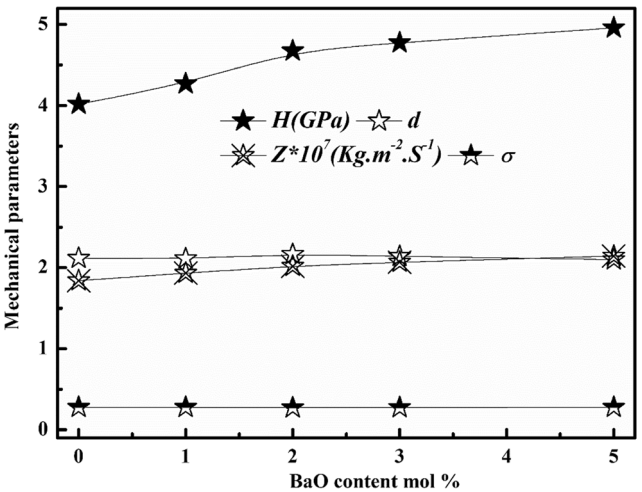

Fig. 9 $H, Z, d, and\ \sigma$ of fabricated glasses

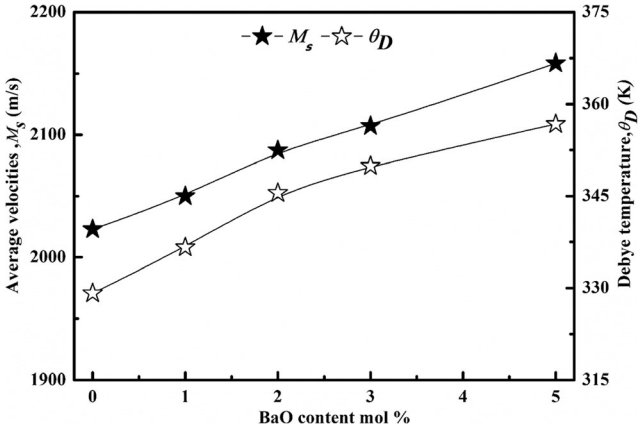

Fig. 10 $M_s and\ \theta_D$ of fabricated glasses

Variations in elastic moduli, on the other hand, can control the amorphous networks. All the experimental ($H, Z, d, \sigma, \theta_D$, $\alpha_P, M_s, V_i\ G_i$) values of elastic moduli of fabricated glasses were collected in Figs. 9, 10, 11 and 12. Variations in elastic moduli are like (V_L) and (V_T) variations. Therefore, these variations were increase as BaO increase. H increase from 4.019 to 4.4958, σ increase from 0.2752 to 0.2766, Z increase from 1.84 to 2.14, θ_D increase from 329.15 to 356.75, α_P increase from 109141.7 to 116682.7,$M_s$increasefrom2022.9 to2158.4, and V_i crease from 0.398 to 0.434. As a result, as the amount of BaO in the glass increases, the structure becomes more rigid and tough. All glass samples had (d) close to 2. This indicates that all the glasses have a two-dimensional layer structure network. Table 4 shows these variations.

3.3 Latent heat of melting ΔH_m, the diffusion constant D_i and Grüneisen factor (ϒ)

When a material is melted, the molecules change state from solid to liquid, and the latent heat of melt is a form of internal or potential energy stored by the melted substance [52]. The diffusion constant is a measurement of molecule mobility that

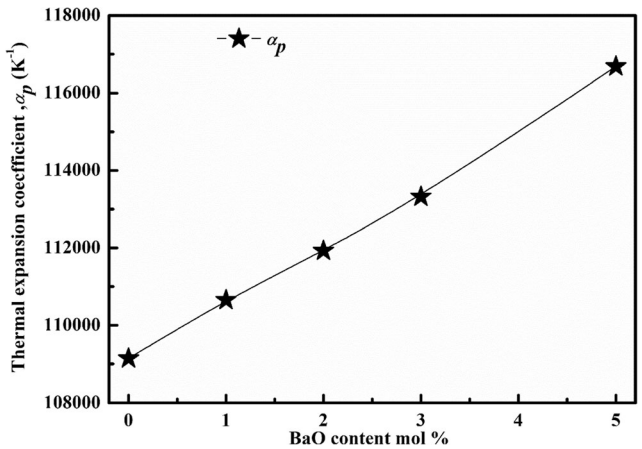

Fig. 11 α_P of fabricated glasses

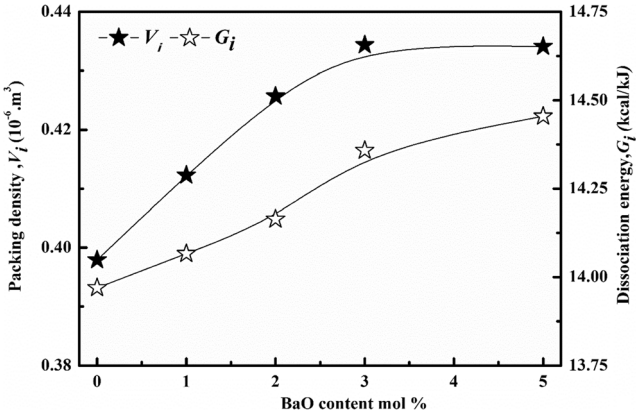

Fig. 12 V_i G_i of fabricated glasses

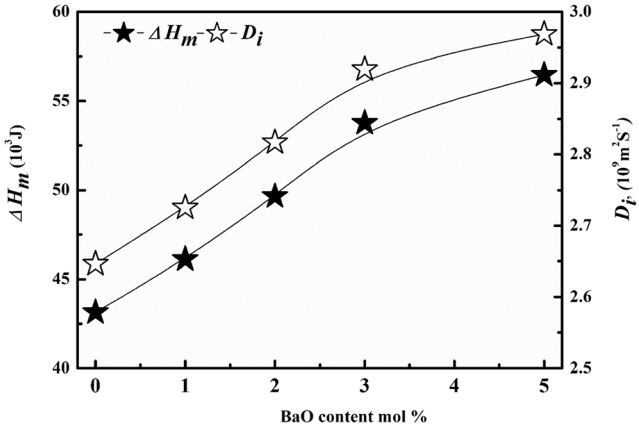

Fig. 13 D_i H_m of fabricated glasses

is determined by the frequency with which the molecule moves and is controlled by the medium's restricting forces. The H_m D_i values were demonstrated in Fig. 13. Table 4 records the H_m D_i values of examined glasses. The values of H_m D_i in the range 42-58(10^3.J) and 2.5-3($10^9 m^2 S^{-1}$) individually. In the fabricated glass samples, H_m D_i increased as BaO increased, due to an increase in the total number of bonds n_b and bridging oxygen (BO). These results are supported with elastic moduli data.

Grüneisen parameter, which connects the characteristic of heat capacity at constant volume, K, α_p, and V_m, is one of the most important quantities in thermodynamics. ϒ increment from 1.629 to 1.64 with increasing BaO as shown in Fig. 14 and lists in Table 4.

T_g and the sound velocity have been shown to be related by Heuer and Spiess [53–56], $T_g = C_g M V_s^2$, where C_g is constant, and M average molecular mass. According to Kanno, H, $T_g / T_m = 2/3$. T_m has been shown to be as $T_m = \frac{MV_m^2 \theta_D^2}{C_s}$, where C_s is constant, and $T_m = \frac{3T_g}{2}$, where T_g *glass trasitio n temperature*. The values of $T_g and T_m$ increase as an increment of BaO concentration. As a result, the fabricated glasses' T_g, T_m, and shear elastic constant exhibit the same behavior. Table 4 records the $T_g and T_m$ values of examined glasses. As a result of the preceding observations, we can deduce that $T_g and T_m$ are strongly related to the elastic constant.

Table 4 Variations in elastic moduli for fabricated glasses

Samples	G 1	G 2	G 3	G 4	G 5
V_i x10^{-6}, (m^3)	0.398	0.412	0.426	0.434	0.434
Gi, (kcal/kJ	13.969	14.067	14.164	14.358	14.455
α_p, (K^{-1})	109142.67	110650.67	111926.67	113318.67	116682.67
d	2.11	2.11	2.16	2.14	2.10
σ	0.275	0.276	0.271	0.273	0.277
$Zx10^7$ ($kg.m^{-2}.s^{-1}$)	1.84	1.93	2.02	2.07	2.14
θ_D, (K)	329.15	336.61	345.51	349.9	356.75
O_{PD}, (mol/L)	18.35	17.78	17.28	17.05	17.12
V_o, (cm^3/mol)	54.48	56.25	57.88	58.64	58.41
H, (GPa)	4.02	4.27	4.67	4.77	4.96
M_s (m. s^{-1})	2022.88	2049.98	2087.4	2107.2	2158.36
ΔH_m	43.13	46.11	49.66	53.76	56.47
D_i	2.65	2.73	2.817	2.92	2.97
ϒ	1.629	1.631	1.61	1.62	1.64
T_g (°C)	489.1	506.8	522.7	540.0	581.6
T_m (°C) according to mechanical	929.3	927.6	938.9	959.0	1033.6
T_m (°C)	733.7	760.2	784.1	810.1	872.4

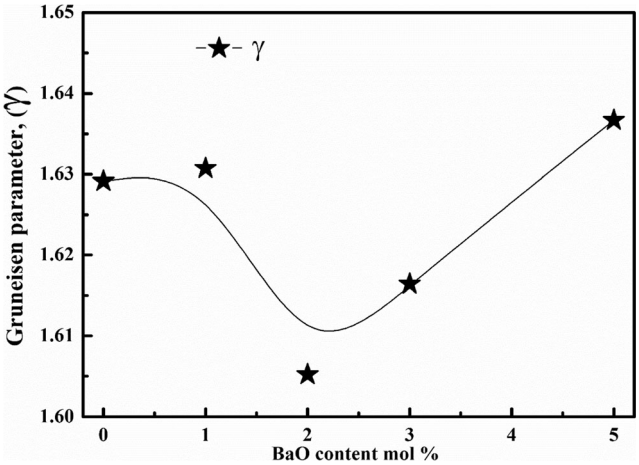

Fig. 14 ϒ of fabricated glasses

4 Conclusions

Using melt-quenching techniques, the glass system $22SiO_2$-$23Bi_2O_3$-$37B_2O_3$-$13TiO_2 - (5 - x)$ LiF- x BaO was prepared. The influences of BaO on the mechanical characteristics of fabricated glasses were investigated in the current article. The fabricated samples are amorphous, according to XRD analysis. In this manuscript, the molar volume is reduced while the density is raised. The ultrasonic velocity elastic moduli of fabricated glasses are mainly affected by changes in glass network connectivity. In the current study, LiF was substituted for BaO because single-bond Ba O energy in the glass network is higher than Li F energy, making these glasses more rigid. Moreover, BaO has a higher average cross-link density than LiF, which contributes to its superiority. Therefore, as BaO levels rise, all the mechanical parameters rise as well. As a result, the fabricated glasses' T_g, T_m, and shear elastic constant exhibit the same behavior. The Latent heat of melting, diffusion constant, and Grüneisen factor have been used to link the mechanical and thermodynamic characteristics of manufactured glass.

Acknowledgements We would like to thank Taif University Research Supporting Project number (TURSP-2020/24), Taif University, Taif, Saudi Arabia. Moreover, the authors express their gratitude to the Deanship of Scientific Research at King Khalid University for funding this work through research groups program under grant number R.G.P. 2/137/42.

Author Contributions Kh. S. Shaaban: Conceptualization, Methodology, Writing Reviewing Discussion and Editing helping in reviewers' responses. Z.A. Alrowaili, Ateyyah M. Al-Baradi, Atif Mossad Ali, E. A. Abdel Wahab, M.S. Al-Buriahi, Editing helping in reviewers' responses.

Data Availability My manuscript and associated personal data.

Declarations The authors declare that they have no known competing financial interests.

Conflict of Interest The authors declare that they have no conflict of interest.

Declaration of Competing Interest The authors declare that they have no known competing financial interests.

Consent to Participate The authors consent to participate.

Consent for Publication The author's consent for publication.

References

1. Zhang L, Kang J, Wang J, Khater GA, Shi Q, Li S, Zhao J, Teng J, Yue Y (2019)Effects of Y_2O_3on structure and dielectric properties of aluminoborosilicate glasses. J Non-CrystSolids 503–504:110–114. https://doi.org/10.1016/j.jnoncrysol.2018.09.032
2. Ruengsri S, Kaewkhao J, Limsuwan P (2012)Optical Characterization of Soda Lime Borosilicate Glass Doped with TiO_2. Procedia Eng 32(2012):772–779. https://doi.org/10.1016/j.proeng.2012.02.011
3. Mahmoud KH, Alsubaie AS, Wahab EAA, Abdel-RahimFM, Shaaban KS (2021)Research on the effects of yttrium on bismuth titanate borosilicate glass system. Silicon. https://doi.org/10.1007/s12633-021-01125-0
4. Shaaban KS, Al-BaradiAM, Wahab EAA (2021)The impact of Y_2O_3on physical and optical characteristics, polarizability, optical basicity, and dispersion parameters of B_2O_3–SiO_2–Bi_2O_3–TiO_2glasses. Silicon. https://doi.org/10.1007/s12633-021-01309-8
5. Al-Baradi AM, Wahab EAA, Shaaban KS (2021)Preparation and Characteristics of B_2O_3–SiO_2–Bi_2O_3–TiO_2–Y_2O_3Glasses and Glass-Ceramics. Silicon. https://doi.org/10.1007/s12633-021-01286-y
6. Moghanian A, Nasiripour S, Miri Z, Hajifathali Z, Hosseini SH, Sajjadnejad M, Aghabarari R, Nankali N, Miri AK, Tahriri M (2021)Structural and in vitro biological evaluation of sol-gelderived multifunctional Ti+4/Sr+2 co-dopedbioactive glass with enhanced properties for bone healing. Ceram Int. https://doi.org/10.1016/j.ceramint.2021.07.113
7. Moghanian A, Koohfar A, Hosseini S, Hosseini SH, Ghorbanoghli A, Sajjadnejad M, Raz M, Elsa M, Sharifianjazi F (2021)Synthesis, characterization and in vitro biological properties of simultaneous co-substitutedTi+4/Li+1 58s bioactive glass. J Non-CrystSolids 561:120740. https://doi.org/10.1016/j.jnoncrysol.2021.120740
8. Rahmani M, Moghanian A, Yazdi MS (2021)The effect of Ag substitution on physicochemical and biological properties of sol-gelderived 60 %SiO2–31 %CaO–4 %P2O5–5 %Li2O (mol%) quaternary bioactive glass. Ceram Int 47:15985–15994. https://doi.org/10.1016/j.ceramint.2021.02.173
9. Moghanian A, Nasiripour S, Hosseini SM, Hosseini SH, Rashvand A, Ghorbanoghli A, Pazhouheshgar A, Sharifian Jazi F (2021)The effect of Ag substitution on physico-chemicaland biological properties of sol-gelderived 60 %SiO2-31 %CaO-4 %P2O5-5 %TiO2 (mol%) quaternary bioactive glass. J Non-CrystSolids 560:120732. https://doi.org/10.1016/j.jnoncrysol.2021.120732
10. Rahmani M, Moghanian A, Saghafi Yazdi M (2021)Synthesis and characterization of in vitro properties and biological behavior of Ag/Lico-doped68S bioactive glass with and without phosphate. J Non-CrystSolids 570:121015. https://doi.org/10.1016/j.jnoncrysol.2021.121015
11. Moghanian A, Nasiripour S, Koohfar A, Sajjadnejad M, Hosseini S, Taherkhani M, Miri Z, Hosseini SH, Aminitabar M, Rashvand A (2021)Characterization, in vitro bioactivity, and biological studies of sol-gel-derived TiO2 substituted 58S bioactive glass. Int J Appl Ceram Technol. https://doi.org/10.1111/ijac.13782
12. Pazhouheshgar A, Haghighatfar Y, Moghanian A (2020)Finite element method and analytical analysis of static and dynamic pull-

ininstability of a functionally graded microplate. J Vib Control. https://doi.org/10.1177/1077546320980208
13. Shaaban KS, Abo-NafSM, Hassouna MEM (2019)Physical and structural properties of lithium borate glasses containing MoO_3. Silicon 11:2421–2428. https://doi.org/10.1007/s12633-016-9519-4
14. Sayed MA, Ali AM, Abd El-RehimAF, Abdel Wahab EA, Shaaban KS (2021)Dispersion parameters, polarizability, and basicity of lithium phosphate glasses. J Electron Mater. https://doi.org/10.1007/s11664-021-08921-9
15. Wahab EAA, Aboraia AM, Shafey AME, Shaaban KS, Soldatov AV (2021)The effect of ZrO_2on the linear and non-linearoptical properties of sodium silicate glass. Opt Quant Electron 53. https://doi.org/10.1007/s11082-021-03164-8
16. El-Rehim AFA, Wahab EAA, Halaka MMA, Shaaban KS (2021)Optical properties of SiO_2–TiO_2–La_2O_3–Na_2O – Y_2O_3glasses and a novel process of preparing the parent glass-ceramics. Silicon. https://doi.org/10.1007/s12633-021-01002-w
17. Scannell G, Barra S, Huang L (2016)Structure and properties of Na_2O-TiO_2-SiO_2glasses: Role of Na and Ti on modifying the silica network. J Non-CrystSolids 448:52–61. https://doi.org/10.1016/j.jnoncrysol.2016.06.028
18. Somaily HH, Shaaban KS, Makhlouf SA, Algarni H, Hegazy HH, Wahab EAA, Shaaban ER (2021)Comparative studies on polarizability, optical basicity and optical properties of lead borosilicate modified with titania. J Inorg Organomet Polym Mater 31:138–150. https://doi.org/10.1007/s10904-020-01650-2
19. Shaaban KS, Wahab EAA, Shaaban ER, Yousef ES, Mahmoud SA (2020)Electronic polarizability, optical basicity, thermal, mechanical and optical investigations of ($65B_2O_3$–$30Li_2O$–$5Al_2O_3$) glasses doped with titanate. J Electron Mater 49:2040–2049. https://doi.org/10.1007/s11664-019-07889-x
20. Shaaban KS, Yousef ES, Mahmoud SA, Wahab EAA, Shaaban ER (2020)Mechanical, structural and crystallization properties in titanate doped phosphate glasses. J Inorg Organomet Polym Mater 30:4655–4663. https://doi.org/10.1007/s10904-020-01574-x
21. Shaaban KS, Koubisy MSI, Zahran HY, Yahia IS (2020)Spectroscopic properties, electronic polarizability, and optical basicity of titanium–cadmiumtellurite glasses doped with different amounts of lanthanum. J Inorg Organomet Polym Mater 30:4999–5008. https://doi.org/10.1007/s10904-020-01640-4
22. El-Rehim AFA, Zahran HY, Yahia IS, Wahab EAA, Shaaban KS (2021)Structural, elastic moduli, and radiation shielding of SiO_2-TiO_2-La_2O_3-Na_2O glasses containing Y_2O_3. J Mater Eng Perform 30:1872–1884. https://doi.org/10.1007/s11665-021-05513-w
23. Strimple JH, Giess EA, (1958), Glass formation and properties of glasses in the system Na_2O-B_2O_3-SiO_2-TiO_2. J Am Ceram Soc 41(7):231-237. https://doi.org/10.1111/j.1151-2916.1958.tb13546.x
24. Limbach R, Karlsson S, Scannell G, Mathew R, Edén M, Wondraczek L (2017)The effect of TiO_2on the structure of Na_2O-CaO-SiO_2glasses and its implications for thermal and mechanical properties. J Non-CrystSolids 471:6–18. https://doi.org/10.1016/j.jnoncrysol.2017.04.013
25. Shaaban KS, Saddeek YB, Sayed MA, Yahia IS, (2018). Mechanical and thermal properties of lead borate glasses containing CaO and NaF. Silicon 10;1973–1978. https://doi.org/10.1007/s12633-017-9709-8
26. Shen Z, Zhao Y, Tian Z, Huang W, Wu J, Lin H (2018)Effect of doping La_2O_3on the structure and properties of the titanium barium silicate glass. J Non-CrystSolids 499:17–24. https://doi.org/10.1016/j.jnoncrysol.2018.07.009
27. Komori K, Yamakawa S, Yamamoto S et al (1994) Glassfiber forming composition, glass fibers obtained from the composition and substrate for circuit board including the glass fibers as reinforcing material, A US, US 5284807
28. Rammah YS, El-AgawanyFI, Elkhoshkhany N, Elmasry F, Reben M, Grelowska I, Yousef E (2021)Physical, optical, thermal, and gamma-rayshielding features of fluorotellurite lithiumniobate glasses: TeO_2-$LiNbO_3$-BaO-BaF_2-La_2O_3J Mater Sci: Mater Electron 32:3743–3752. https://doi.org/10.1007/s10854-020-05119-3
29. Elbatal FHA, Marzouk MA, Hamdy YM, Elbatal HA (2014)Optical and FT infrared absorption spectra of 3d transition metal ions doped in NaF-CaF_2-B_2O_3glass and effects of gamma irradiation. J Solid-StatePhys 2014:1–8. https://doi.org/10.1155/2014/389543
30. El-Rehim AFA, Shaaban KS (2021)Influence of La_2O_3content on the structural, mechanical, and radiation-shieldingproperties of sodium fluoro lead barium borate glasses. J Mater Sci: Mater Electron 32:4651–4671. https://doi.org/10.1007/s10854-020-05204-7
31. Shaaban KS, Alomairy S, Al-BuriahiMS (2021)Optical, thermal and radiation shielding properties of B_2O_3–NaF–PbO–BaO–La_2O_3glasses. J Mater Sci: Mater Electron. https://doi.org/10.1007/s10854-021-05885-8
32. Gaddam A, Fernandes HR, Doumert B, Montagne L, Ferreira JMF (2017)Structure and thermal relaxation of network units and crystallization of lithium silicate-basedglasses doped with oxides of Al and B. Phys Chem Chem Phys 19:26034–26046. https://doi.org/10.1039/c7cp01690e
33. Makishima A, Mackenzie JD (1973)Direct calculation of Young's moidulus of glass. J Non-CrystSolids 12:35–45. https://doi.org/10.1016/0022-3093(73)90053-7
34. Makishima A, Mackenzie JD (1975)Calculation of bulk modulus, shear modulus and Poisson's ratio of glass. J Non-CrystSolids 17:147–157. https://doi.org/10.1016/0022-3093(75)90047-2
35. El-Rehim AFA, Ali AM, Zahran HY, Yahia IS, Shaaban KS (2021)Spectroscopic, structural, thermal, and mechanical properties of B_2O_3-CeO_2-PbO_2glasses. J Inorg Organomet Polym Mater 31:1774–1786. https://doi.org/10.1007/s10904-020-01799-w
36. Shaaban KS, Zahran HY, Yahia IS, Elsaeedy HI, Shaaban ER, Makhlouf SA, Wahab EAA, Yousef ES (2020)Mechanical and radiation-shieldingproperties of B_2O_3–P_2O_5–Li_2O–MoO_3glasses. Appl Phys A 126. https://doi.org/10.1007/s00339-020-03982-9
37. Wahab EAA, Shaaban KS (2018)Effects of SnO_2on spectroscopic properties of borosilicate glasses before and after plasma treatment and its mechanical properties. Mater Res Express 5(2):025207. https://doi.org/10.1088/2053-1591/aaaee8
38. Shaaban KS, Abdel Wahab EA, El-MaarefAA, Abdelawwad M, Shaaban ER, Yousef ES, Wilke H, Hillmer H, Börcsök J (2020)Judd–Ofeltanalysis and physical properties of erbium modified cadmium lithium gadolinium silicate glasses. J Mater Sci: Mater Electron 31:4986–4996. https://doi.org/10.1007/s10854-020-03065-8
39. Saudi HA, Abd-AllahWM, Shaaban KS (2020)Investigation of gamma and neutron shielding parameters for borosilicate glasses doped europium oxide for the immobilization of radioactive waste. J Mater Sci: Mater Electron 31:6963–6976. https://doi.org/10.1007/s10854-020-03261-6
40. Fayad AM, Shaaban KS, Abd-AllahWM, Ouis M (2020)Structural and optical study of CoO doping in borophosphate host glass and effect of gamma irradiation. J Inorg Organomet Polym Mater 30:5042–5052. https://doi.org/10.1007/s10904-020-01641-3
41. Abd-Allah WM, Saudi HA, Shaaban KS, Farroh HA (2019)Investigation of structural and radiation shielding properties of $40B_2O_3$–30PbO–(30-x) BaO-xZnO glass system. Appl Phys A 125. https://doi.org/10.1007/s00339-019-2574-0
42. El-Rehim AFA, Zahran HY, Yahia IS, Ali AM, Shaaban KS (2020)Physical, radiation shielding and crystallization properties of Na_2O-Bi_2O_3- MoO_3-B_2O_3- SiO2-Fe_2O_3glasses. Silicon. https://doi.org/10.1007/s12633-020-00827-1
43. El-Rehim AFA, Wahab EAA, Halaka MMA, Shaaban KS (2021)Optical properties of SiO_2–TiO_2–La_2O_3–Na_2O –

Y_2O_3glasses and a novel process of preparing the parent glass-ceramics. Silicon. https://doi.org/10.1007/s12633-021-01002-w
44. Shaaban KS, Boukhris I, Kebaili I, Al-BuriahiMS (2021)Spectroscopic and attenuation shielding studies on B_2O_3-SiO_2-LiF-ZnO-TiO_2glasses. Silicon. https://doi.org/10.1007/s12633-021-01080-w
45. Abdel Wahab EA, Shaaban KS, Yousef ES (2020)Enhancement of optical and mechanical properties of sodium silicate glasses using zirconia. Opt Quant Electron 52. https://doi.org/10.1007/s11082-020-02575-3
46. Shaaban KS, Wahab EAA, Shaaban ER, Yousef ES, Mahmoud SA (2020)Electronic polarizability, optical basicity and mechanical properties of aluminum lead phosphate glasses. Opt Quant Electron 52. https://doi.org/10.1007/s11082-020-2191-3
47. Shaaban KS, Yousef ES, Abdel Wahab EA, Shaaban ER, Mahmoud SA (2020)Investigation of crystallization and mechanical characteristics of glass and glass-ceramicwith the compositions xFe_2O_3-$35SiO_2$-$35B_2O_3$-$10Al_2O_3$-(20–x) Na_2O. J Mater Eng Perform 29:4549–4558. https://doi.org/10.1007/s11665-020-04969-6
48. Shaaban KS, Abo-NafSM, Abd Elnaeim AM, Hassouna MEM (2017)Studying effect of MoO_3on elastic and crystallization behavior of lithium diborate glasses. Appl Phys A 123. https://doi.org/10.1007/s00339-017-1052-9
49. Shaaban KS, Yousef ES (2020)Optical properties of Bi_2O_3doped boro tellurite glasses and glass ceramics. Optik 203:163976. https://doi.org/10.1016/j.ijleo.2019.163976
50. El-Rehim AFA, Zahran HY, Yahia IS, Makhlouf SA, Shaaban KS (2021)Radiation, crystallization, and physical properties of cadmium borate glasses. Silicon 13:2289–2307. https://doi.org/10.1007/s12633-020-00798-3
51. Raouf El-MallawanyYS, Rammah, Eladawy A, (2021), A study of thermal, optical and mechanical properties of some tellurite glasses, Thesis for: Master degree. https://doi.org/10.13140/RG.2.2.13343.48802
52. Heuer A, Spiess HW (1994)Universality of the glass transition temperature. J Non-CrystSolids 176:294–298. https://doi.org/10.1016/0022-3093(94)90090-6
53. Gupta NP (1973)On the Lindemann law of melting of solids. Solid State Commun 13:69–71. https://doi.org/10.1016/0038-1098(73)90069-0
54. Jabraoui H, Vaills Y, Hasnaoui A, Badawi M, Ouaskit S (2016)Effect of sodium oxide modifier on structural and elastic properties of silicate glass. J Phys Chem B 120(51):13193–13205. https://doi.org/10.1021/acs.jpcb.6b09664
55. Kanno H (1981)A simple derivation of the empirical rule. J Non-CrystSolids 44:409–413. https://doi.org/10.1016/0022-3093(81)90047-8
56. Hruby A (1972)Evaluation of glass-formingtendency by means of DTA. Czech J Phys 22:1187–1193. https://doi.org/10.1007/BF01690134